Characteristic-based-split (CBS) algorithm for incompressible flow problems with heat transfer

Received July 1998
Accepted August 1998

N. Massarotti
Dipartimento di Ingegneria Industriale, Università degli studi di Cassino, Cassino, Italy, and
P. Nithiarasu and O.C. Zienkiewicz
Institute for Numerical Methods in Engineering, Department of Civil Engineering, University of Wales Swansea, Swansea, UK

Introduction

Analysis of fluid flow and heat transfer is important due to many engineering applications such as thermal insulation, cooling of electronic equipments, solar energy devices, nuclear reactors etc. An extensive study on fundamental fluid flow and heat transfer problems is necessary in order to design these heat transfer equipments. For most of the thermal flow applications, the fluid can be considered incompressible and Navier-Stokes equations represent the mathematical model of the reality. To achieve a proper understanding of a physical problem via numerical solution of the governing equations, it is essential to use an algorithm which is reliable. In our earlier papers[1-4], we have presented a general algorithm for the solution of both compressible and incompressible Navier-Stokes equations.

Finite element method has been used for the solution of Navier-Stokes equations since the early 1970s[5-7]. The standard Bubnov-Galerkin method, being equivalent to a central difference approximation, when applied to convection dominated problems produces a solution with oscillations or "wiggles"[5]. Such unrealistic solutions were eliminated via many stabilization schemes in finite elements[8-10] inspired by the upwinding techniques of FDM[11,12]. Initially the desired effect was achieved owing to Petrov-Galerkin type weighting functions[8-10], thus increasing not only the stability but also the accuracy of the solution. Once an analogy between upwinding and the so-called balancing diffusion was established, other procedures were proposed, where an artificial diffusion is added to the equation so permitting the standard Galerkin method to be used[13,14]. However schemes such as the Taylor-Galerkin[15] or the characteristic Galerkin[16] method have shown that balancing diffusion emerges naturally when the equations are discretized in

This research has been partially supported by NASA grant NAGW/2127, AMES Control Number 90-144.

International Journal of Numerical Methods for Heat & Fluid Flow
Vol. 8 No. 8, 1998, pp. 969-990.

time. In particular in the characteristic Galerkin method the temporal derivative is discretized along the characteristic, where the equation is self-adjoint in nature and thus the Galerkin spatial approximation is optimal.

Another difficulty, which arises when the Galerkin finite element method is used to solve incompressible (or slightly compressible) Navier-Stokes equations, is due to the zero diagonal term present in the discretized equations. Penalty forms introduce a small term in the diagonal, so avoiding the singularity of the equations, but still the Babŭska-Brezzi conditions have to be satisfied a priori and so penalty forms can be applied only with reduced integration[5]. Other methods have been proposed to avoid these restrictions using particular weighting procedures[17,18]. Nevertheless, as it has been observed by Scheider *et al.*[19], Kawahara and Ohmiya[20], and then shown by Zienkiewicz and Wu[21], these restrictions are avoided naturally through some time stepping procedures. One of these is the operator splitting scheme, on which the present algorithm is based, that was initially introduced by Chorin[22] in the finite difference context, and then adopted to finite elements[19-21,23,24]. The method is based on the calculation of an intermediate velocity from a momentum equation where the pressure gradients are omitted; the pressure is then evaluated from an equation of Laplacian form (Poisson equation). Finally the velocity is corrected using the computed pressures. When the steady state is reached the discretized equations, instead of the zero term, have a diagonal term proportional to the time increment. This allows arbitrary order interpolation functions for velocity and pressure.

In this work equal-order interpolation functions have been used for all the variables and the algorithm has been used in its semi-implicit form[1-3,24]. The simplex linear triangular elements are used to divide the domain into finite elements. The solution of benchmark problems, such as natural convection in a cavity and laminar flow over a backward facing step for forced convection, show the excellent accuracy of the scheme. Further, this has been confirmed when the algorithm has been used to solve some practical problems for which the agreement with the experiment is excellent.

Governing equations

The governing equations for incompressible viscous flow in their dimensionless form are given here. Invoking the Boussinesq approximation, the equations in two dimensions are

continuity equation:

$$\frac{\partial u_i}{\partial x_i} = 0 \tag{1}$$

momentum equation:

$$\frac{\partial u_i}{\partial t} = -\frac{\partial u_j u_i}{\partial x_j} - \frac{\partial p}{\partial x_i} + \frac{\partial \tau_{ij}}{\partial x_i} + \gamma RaPr\, T \tag{2}$$

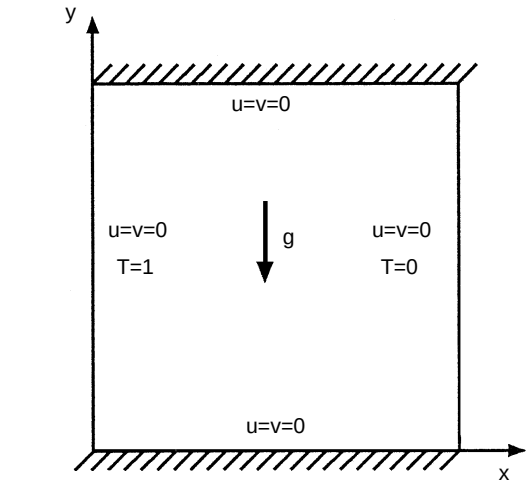

(a)

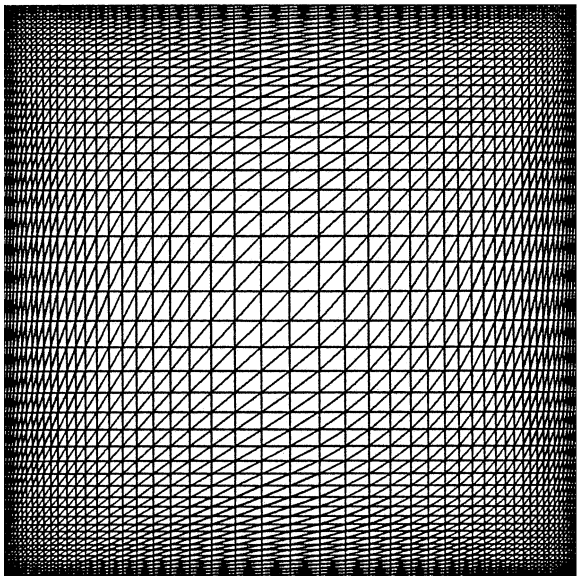

(b)

Figure 1.
Buoyancy driven flow in a square cavity: (a) domain and boundary conditions; (b) finite element mesh, no. nodes 2,601; no. elements 5,000

energy equation:

$$\frac{\partial T}{\partial t} = -\frac{\partial u_i T}{\partial x_i} + \frac{\partial^2 T}{\partial x_i^2} \tag{3}$$

defined in $\Omega \times [0,t]$ with $\Omega \subset \Re^2$ domain of interest.

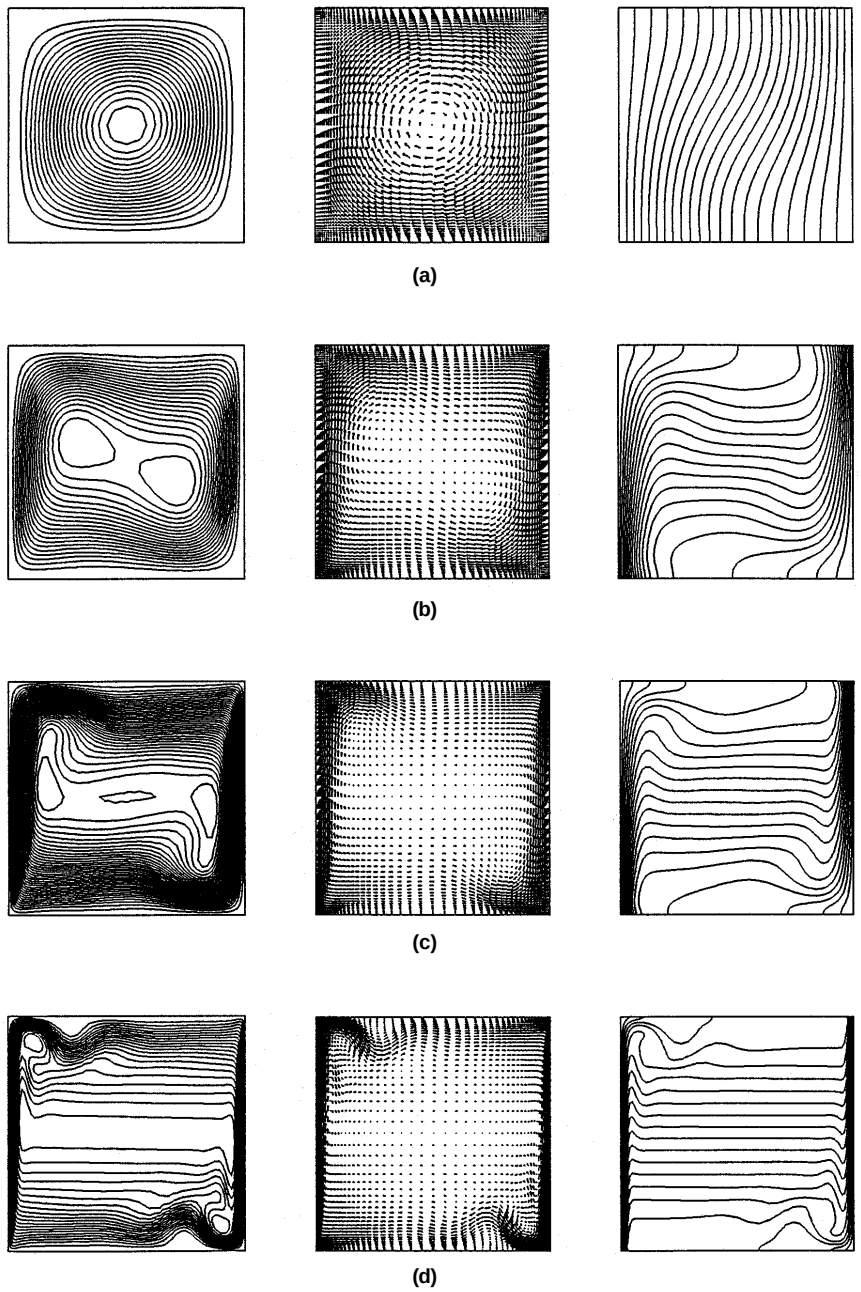

Figure 2.
Stream lines (left), velocity vectors (middle) and isotherms (right) for different Rayleigh numbers:
(a) Ra = 10^3;
(b) Ra = 10^5;
(c) Ra = 10^6;
(d) Ra = 4×10^7

In the equations above $u_i = (u_1,u_2)$ is the velocity components, p is the pressure, γ is the vector equal to unity in vertical direction and zero in horizontal

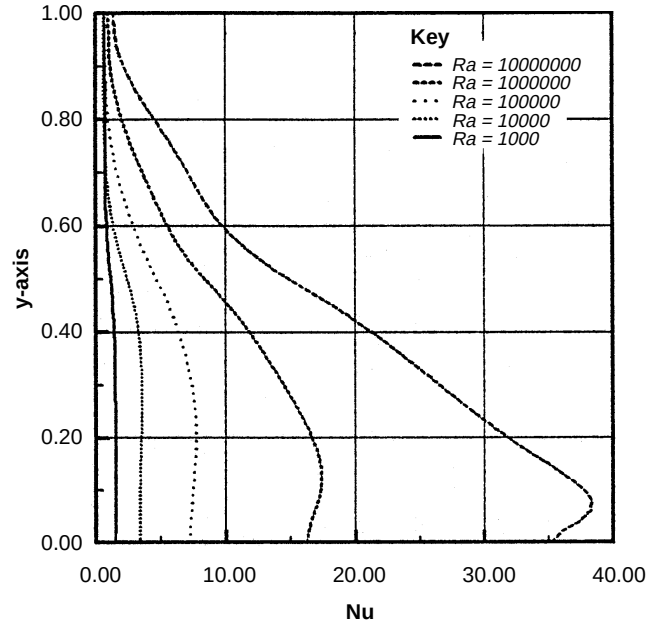

(a)

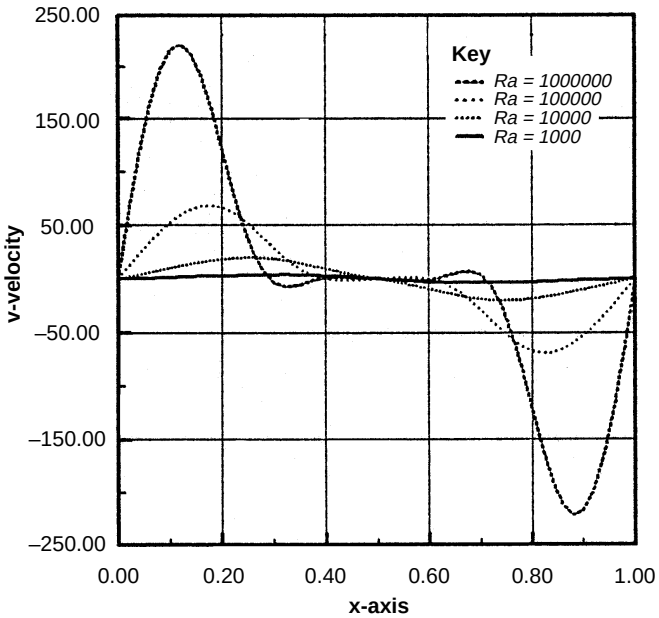

(b)

Figure 3.
(a) Local Nusselt number distribution along the hot wall; (b) vertical velocity distribution at mid-height along x-direction

Ra	Nu			Ψ_{vmax}			v_{max}		
	[26]	[27]	Present	[26]	[27]	Present	[26]	[27]	Present
10^3	1.116	1.118	1.117	1.174	1.175	1.167	3.696	3.697	3.692
10^4	2.243	2.245	2.243	5.081	5.074	5.075	19.64	19.63	19.63
10^5	4.517	4.522	4.521	9.121	9.619	9.153	68.68	68.64	68.85
10^6	8.797	8.825	8.806	16.41	16.81	16.49	221.3	220.6	221.6
10^7	–	16.52	16.40	–	30.17	30.33	–	699.3	702.3
4×10^7	–	23.78	23.64	–	–	43.12	–	–	1417

Sources: [26,27]

Table I.
Natural convection in a square cavity: comparison with benchmark solution

direction, T the temperature of the fluid, Pr the Prandtl number, Ra the Rayleigh number and τ is the shear stress tensor, given by:

$$\tau_{ij} = Pr\left(\frac{\partial u_i}{\partial x_j} + \frac{\partial u_j}{\partial x_i} - \frac{2}{3}\frac{\partial u_k}{\partial x_k}\delta_{ij}\right) \qquad i,j = 1,2 \tag{4}$$

where δ_{ij} is the Kronecker delta.

The following scales and nondimensional parameters are used in the above governing equations:

$$x_i = \frac{x_i^*}{L}\,, \qquad u_i = \frac{u_i^*}{\alpha/L}\,, \qquad p = \frac{p^*}{\rho\alpha^2/L^2}\,, \qquad t = \frac{t^*}{L^2/\alpha}$$

$$T = \frac{(T^* - T_c)}{(T_h - T_c)}\,, \quad Pr = \frac{\mu}{\rho\,\alpha}\,, \quad Ra = \frac{g\,\beta\,(T_h - T_c)\,L^3}{\nu\,\alpha} \tag{5}$$

where $x_i = (x_1, x_2)$ represent the coordinate axes, ρ is the density, α the thermal diffusivity and μ the dynamic viscosity of the fluid; T_h, T_c and L are respectively the higher, lower temperatures and the characteristic length of the problem examined. The asterisk has been used for the dimensional variables.

When forced convection dominates the process different scales and parameters are introduced, such as:

$$x_i = \frac{x_i^*}{L}\,, \qquad u_i = \frac{u_i^*}{\bar{U}}\,, \qquad p = \frac{p^*}{\rho\,\bar{U}^2}\,, \qquad t = \frac{t^*}{L^2/\alpha}$$

$$T = \frac{(T^* - T_c)}{(T_h - T_c)}\,, \quad Pr = \frac{\mu}{\rho\,\alpha}\,, \quad Re = \frac{\rho\,\bar{U}\,D}{\mu} \tag{6}$$

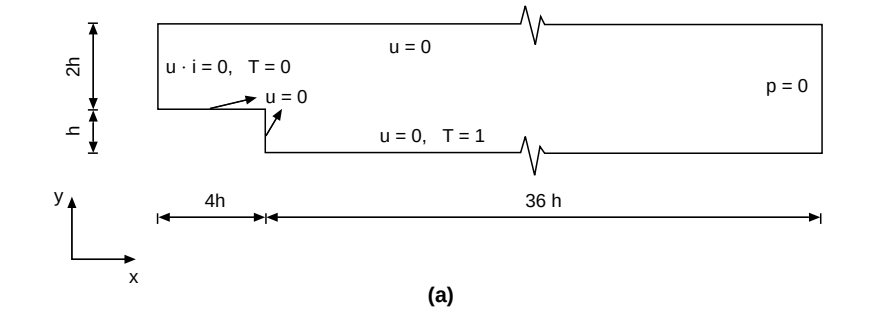

(a)

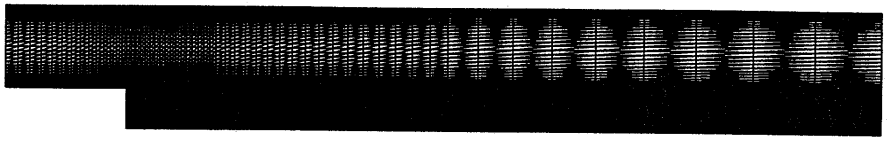

(b)

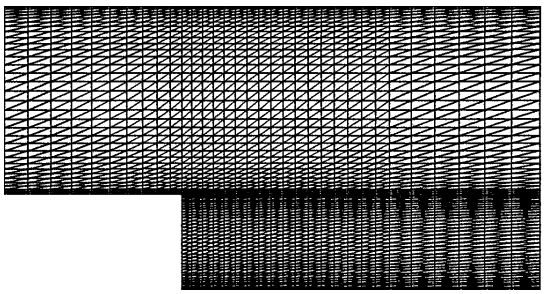

(c)

Figure 4.
Flow over a backward facing step: (a) domain and boundary conditions; (b) finite element mesh, no. nodes: 4,183, no. elements: 8,092; (c) mesh near the step

where $\overline{U}$ is the free stream velocity, Re is the Reynolds number. Appropriate scalings are used dependent on the nature of the problem considered.

Characteristic-based-split algorithm (CBS)

In this section, we give the essential steps of the CBS algorithm. The Galerkin spatial approximation can be found in detail elsewhere[5], and is not discussed here. As we deal with incompressible problems, the semi-implicit form of the algorithm has been used. We shall consider only the case where $\theta_1 = 1$ and $\theta_2 = 1$ (see[1]). The four essential steps of this algorithm are:

step 1, calculation of intermediate momentum

$$\tilde{u}_i^{n+1} = u_i^n + \Delta t \left[-\frac{\partial (u_i u_j)}{\partial x_j} + \frac{\partial \tau_{ij}}{\partial x_j} - f_i + \frac{\Delta t}{2} u_k \frac{\partial^2}{\partial x_k \partial x_j} (u_i u_j) \right]^n \quad (7)$$

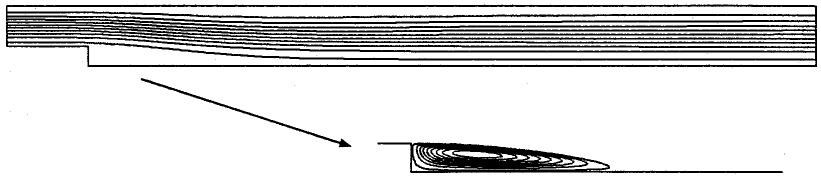

(a) streamlines

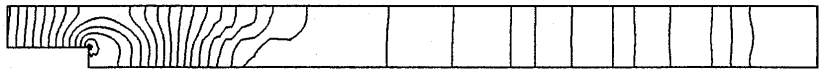

(b) pressure contours

(c) isotherms

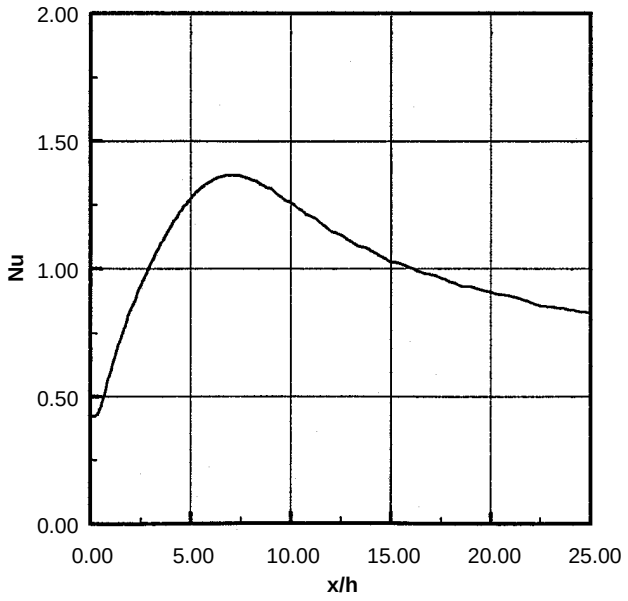

(d) hot wall local Nusselt number

Figure 5.
Stream lines, pressure, isotherm and local Nusselt number distribution for Re = 100

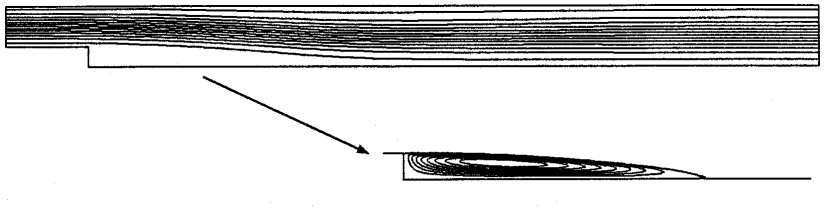

(a) streamlines

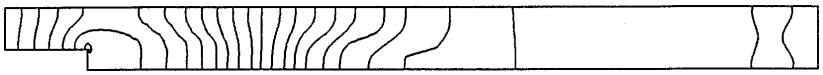

(b) pressure contours

(c) isotherms

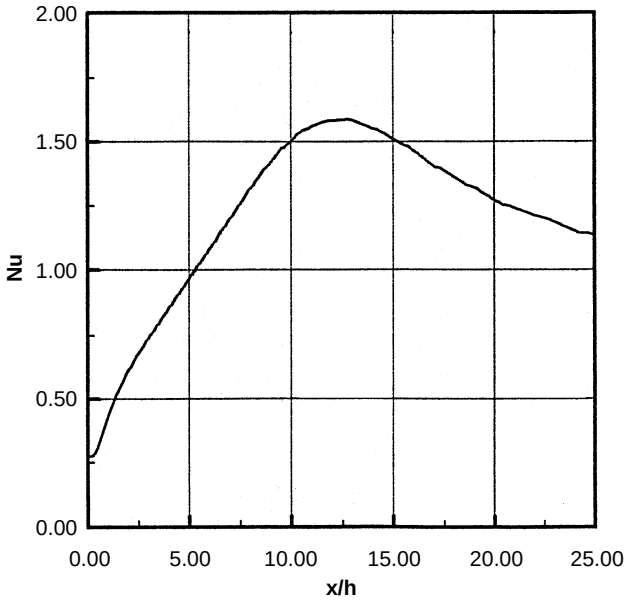

(d) hot wall local Nusselt number

Figure 6.
Stream lines, pressure, isotherm and local Nusselt number distribution for Re = 229

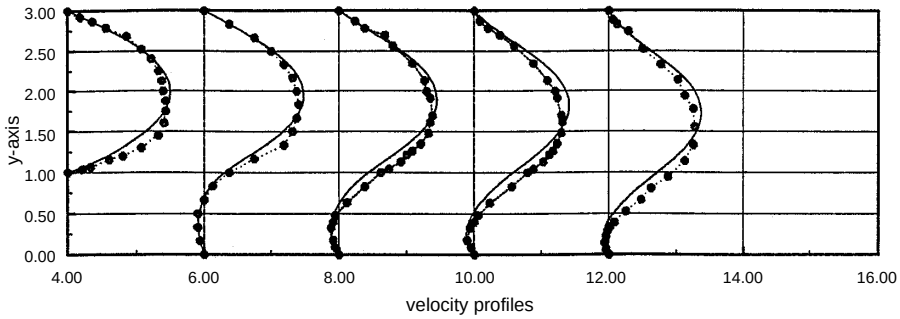

(a)

Source: [28]

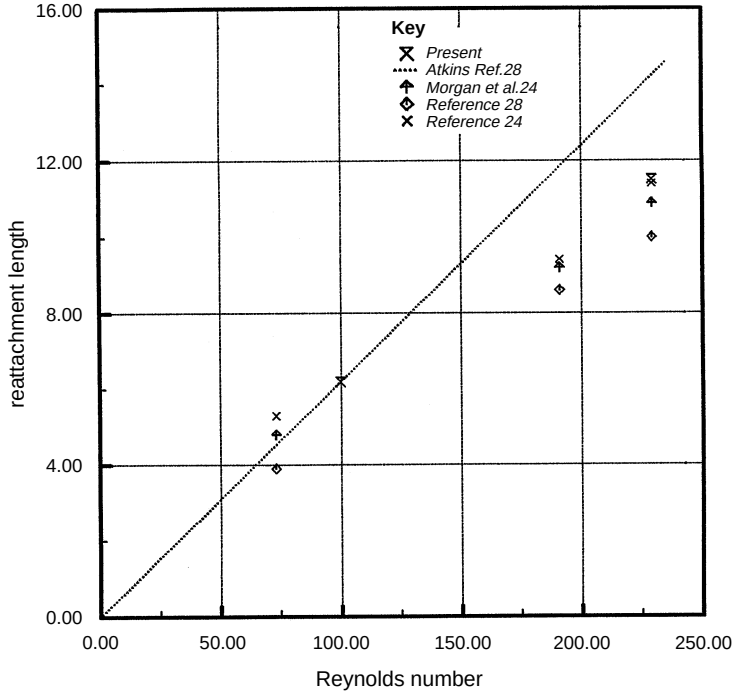

(b)

Figure 7.
Comparison of present predictions with experimental and theoretical data:
(a) velocity profile at different sections;
(b) reattachment length

step 2, calculation of pressure field

$$\left(\frac{\partial^2 p}{\partial x_i \partial x_j}\right)^{n+1} = \frac{1}{\Delta t}\left[\frac{\partial \tilde{u}_i}{\partial x_i}\right] \tag{8}$$

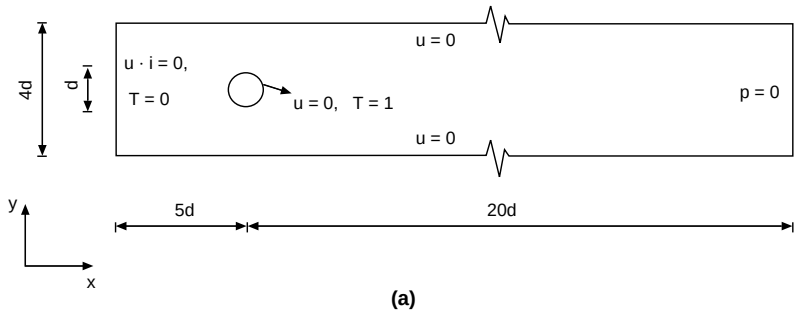

(a)

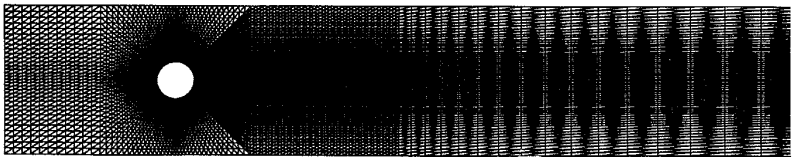

(b)

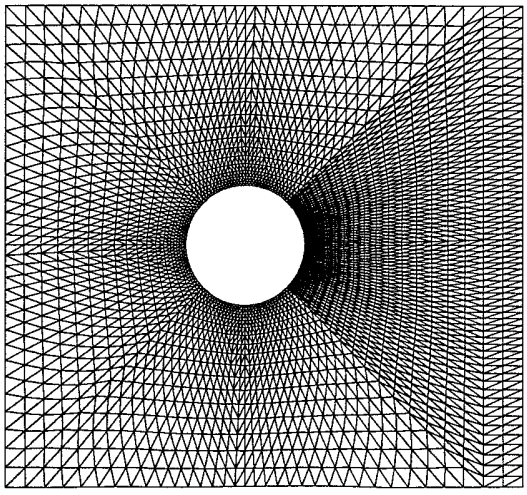

(b)

Figure 8.
Vortex shedding downstream a cylinder: (a) domain and boundary conditions; (b) finite element mesh, no. nodes: 5,944; no. elements: 11,456; (c) mesh near the cylinder

step 3, velocity correction

$$u_i^{n+1} = \tilde{u}_i^n - \Delta t \left[\frac{\partial p}{\partial x_i}\right]^{n+1} \tag{9}$$

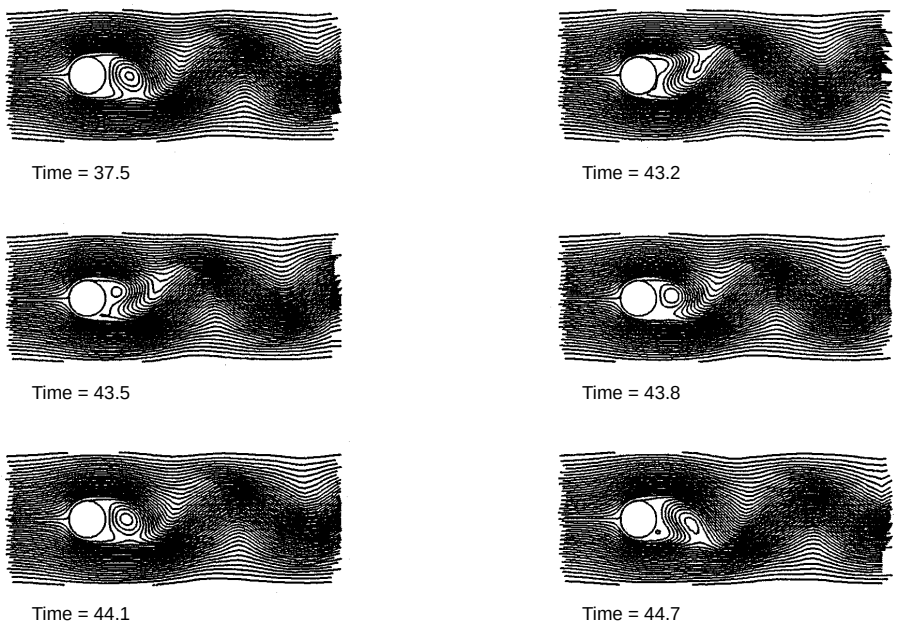

Figure 9.
Vortex shedding behind a cylinder, Re = 200

step 4, energy equation

$$T^{n+1} = T^n + \Delta t \left(-\frac{\partial (u_i T)}{\partial x_i} + \frac{\partial^2 T}{\partial x_i \partial x_j} + \frac{\Delta t}{2} u_j \frac{\partial^2}{\partial x_i \partial x_j} (u_i T) \right)^n . \quad (10)$$

where $\tilde{u}$ is the intermediate velocity. The algorithm in this form is conditionally stable. The critical time step given by: $\Delta t_{crit} = h/|u|$[24] which is from the linear stability analysis of one dimensional convection-diffusion equation[25].

Numerical examples

In this section a variety of test problems have been presented in order to prove the capability of the present algorithm. Some benchmark examples and few

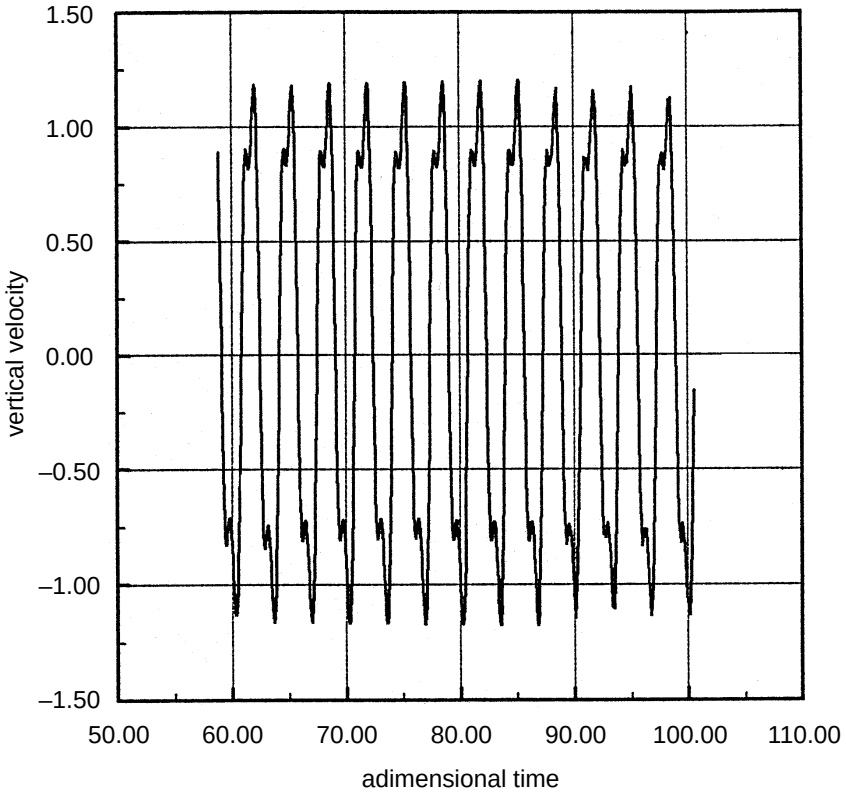

Figure 10. Vortex shedding behind a cylinder, Re = 200, vertical velocity distribution with time at a point 4.5d downstream the cylinder

more difficult heat transfer problems are solved in this study. The fluid considered is air in all the example problems.

Natural convection in a square cavity

The first example presented is the buoyancy-driven flow in an square cavity which is a standard test case for validating algorithms and computer codes which are concerned with the solution of thermal flow problems.

The problem definition and the mesh used for the calculation are shown in Figure 1. Both the horizontal walls are assumed to be thermally insulated, and the vertical sides are kept at different temperatures. For the velocity, no-slip conditions are assumed to prevail on all the walls of the cavity. A wide range of Rayleigh numbers from 10^3 to 4×10^7 are studied and the results for the steady state solution are presented in Figures 2 and 3. It is seen that the steady-state solution presented in these figures are symmetric with respect to the center of the cavity and is in excellent agreement with the benchmark solution[26] and other available results. Table I shows the comparison of quantitative results with the available benchmark solutions. It is seen that the agreement is excellent even at higher Rayleigh numbers.

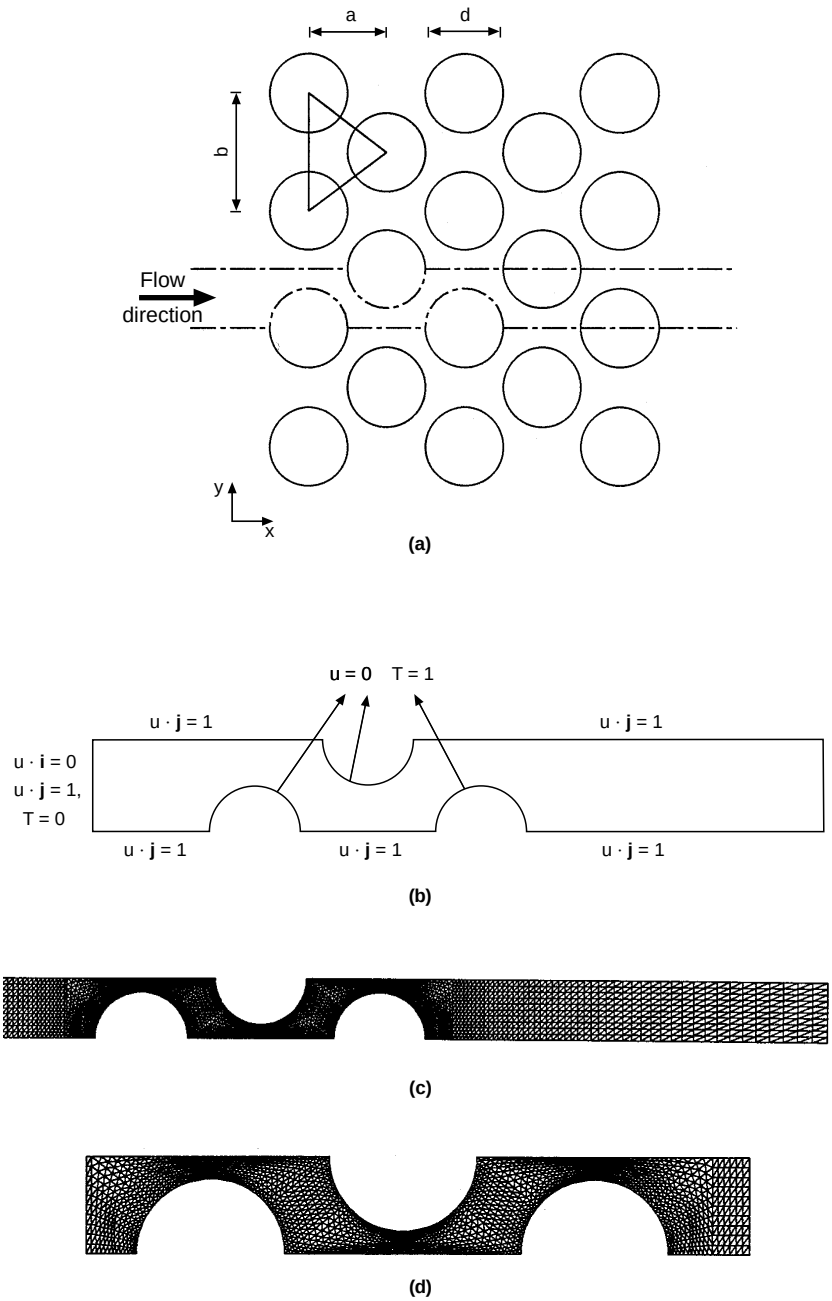

Figure 11.
(a) Flow past a tube bank; (b) formulation and boundary conditions (three cylinders); (c) finite element mesh, no. nodes: 2,162; no. elements: 3,948; (d) mesh near the cylinders

Laminar flow and heat transfer over a downstream facing step

This is the second bench-mark to validate the forced flow and heat transfer. Unlike the buoyancy-driven flow here the momentum and energy equations are

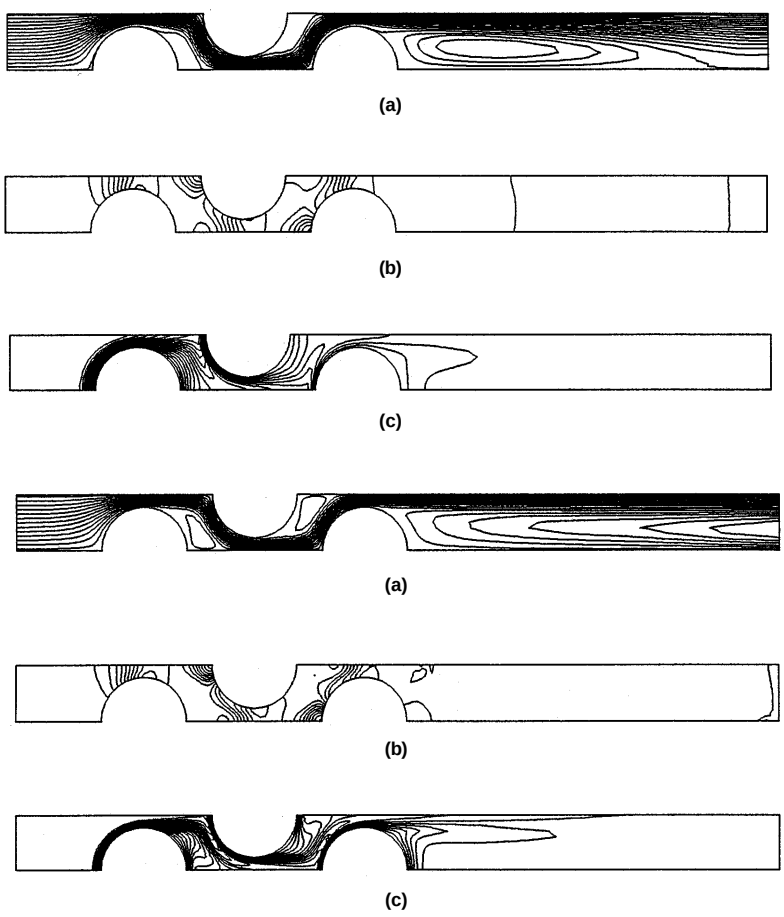

Figure 12.
Flow past a tube bank at Re = 50 (three cylinders): (a) stream lines; (b) pressure contours; (c) isotherms

Figure 13.
Flow past a tube bank at Re = 150 (three cylinders): (a) stream lines; (b) pressure contours; (c) isotherms

not coupled, but the convective terms become stronger. The problem definition and mesh are shown in Figure 4, and the height of the step is the characteristic length. A laminar flow is considered to enter the domain at inlet section placed four times the step height before the enlargement. The inlet velocity profile is parabolic and the Re is based on the average velocity at the inlet. The total length of the domain is taken equal to 40 times the step height so that the zero pressure at exit is valid (traction free boundary conditions for the pressure); free boundary conditions were assumed for all the other variables. All the walls of the duct are insulated except the lower one downstream the step, which is kept at a constant temperature higher than that of the fluid at the inlet. Figures 5, 6 and 7 present the results for Reynolds numbers 100 and 229. In general solution is smooth even at a Reynolds number of 229. The heat transfer results are in good agreement with those of Kondon *et al.*[29]. The comparison of present predictions (Figure 10) with the experiment of Denham and Patrick[28], has small deviations and this can be attributed to the influence of the inlet velocity

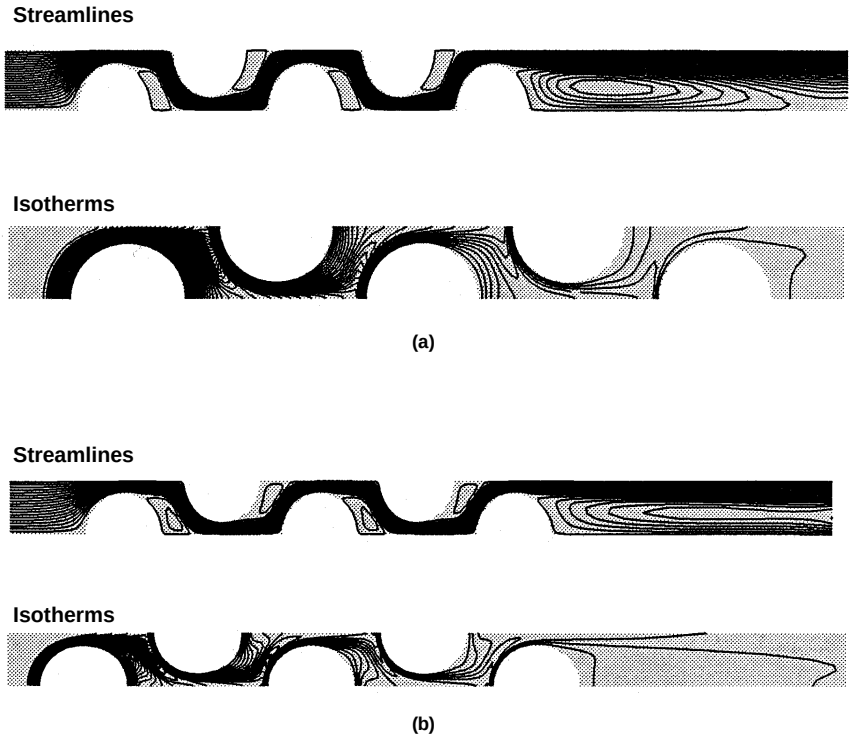

Figure 14.
Flow past a tube bank (five cylinders): (a) stream line and isotherm patterns (Re = 50); (b) stream line and isotherm patterns (Re = 150)

profile. In fact the experimental data are not generated from an exactly parabolic inlet velocity profile.

Vortex shedding behind a circular cylinder

The domain studied and the finite element mesh around the cylinder are shown in Figure 8. The inlet velocity is assumed to have a parabolic profile. On the outer walls of the domain, no-slip conditions are assumed and are also thermally insulated. The cylinder on the flow path is assumed to be at a higher temperature than that of the incoming fluid. Also zero velocity components are imposed on it. Free boundary condition for the outlet flow has been "imposed" for all the variables except the pressure which is equal to zero. In this problem after an initial phase, the flow starts separating and symmetric eddies form behind the cylinder. After a certain time a periodic process of formation of vortices has been observed. The distribution of the streamlines in Figure 9 shows the formation of vortices behind the cylinder at different non-dimensional times; in the same figure a sample of distributions of the pressure and of the isotherms are also given. Figure 10 shows the time dependence of the vertical velocity 4.5 diameters downstream the cylinder.

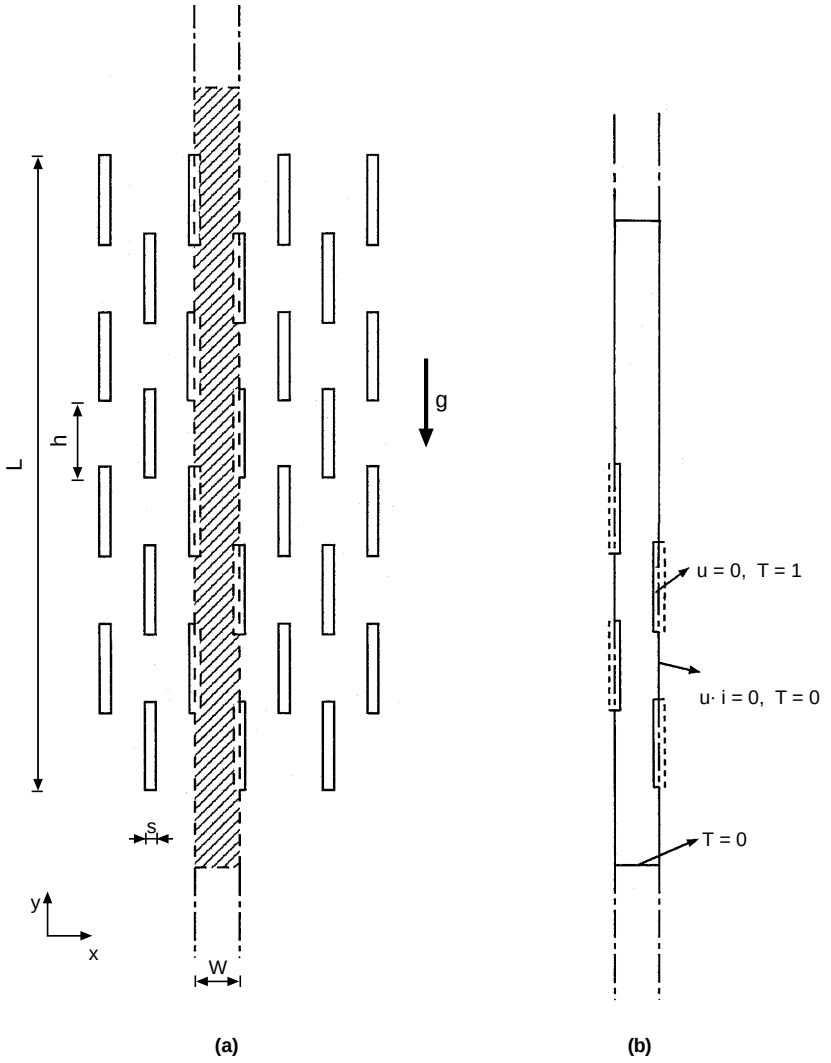

Figure 15.
(a) Natural convection from an array of hot staggered plates; (b) formulation and boundary conditions

Heat transfer from tube banks

Study of flow over tube bundles is important due to its application like heat exchanger. Here, as in many other design problems the data of a numerical simulation can save a lot of time. The geometry considered and the grid generated are shown in Figure 11. The same outflow boundary conditions are applied as in the last two examples. The calculation was performed for different Reynolds numbers and Figures 12, 13 and 14 present the results. As already seen the algorithm permits to obtain a very smooth solution for the pressure even when the convection increases.

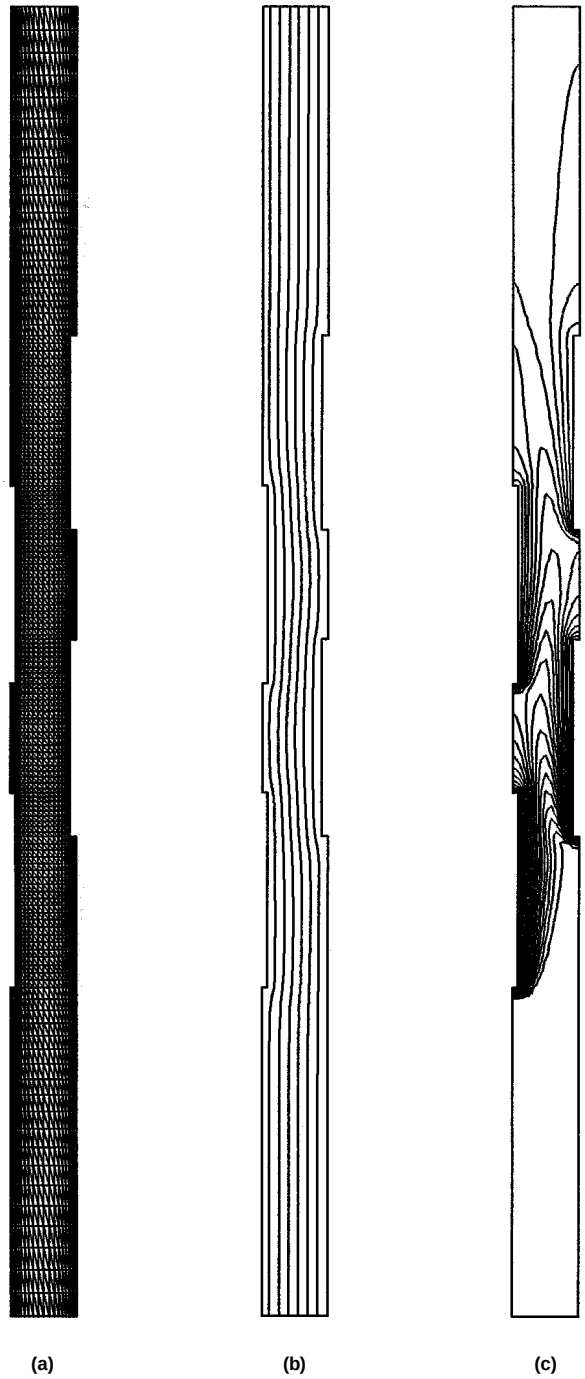

Figure 16.
Staggered plates,
$W = 0.1$, $Ra = 5 \times 10^5$:
(a) finite element mesh,
no. nodes: 2,640,
no. elements: 4,928;
(b) stream lines;
(c) isotherms

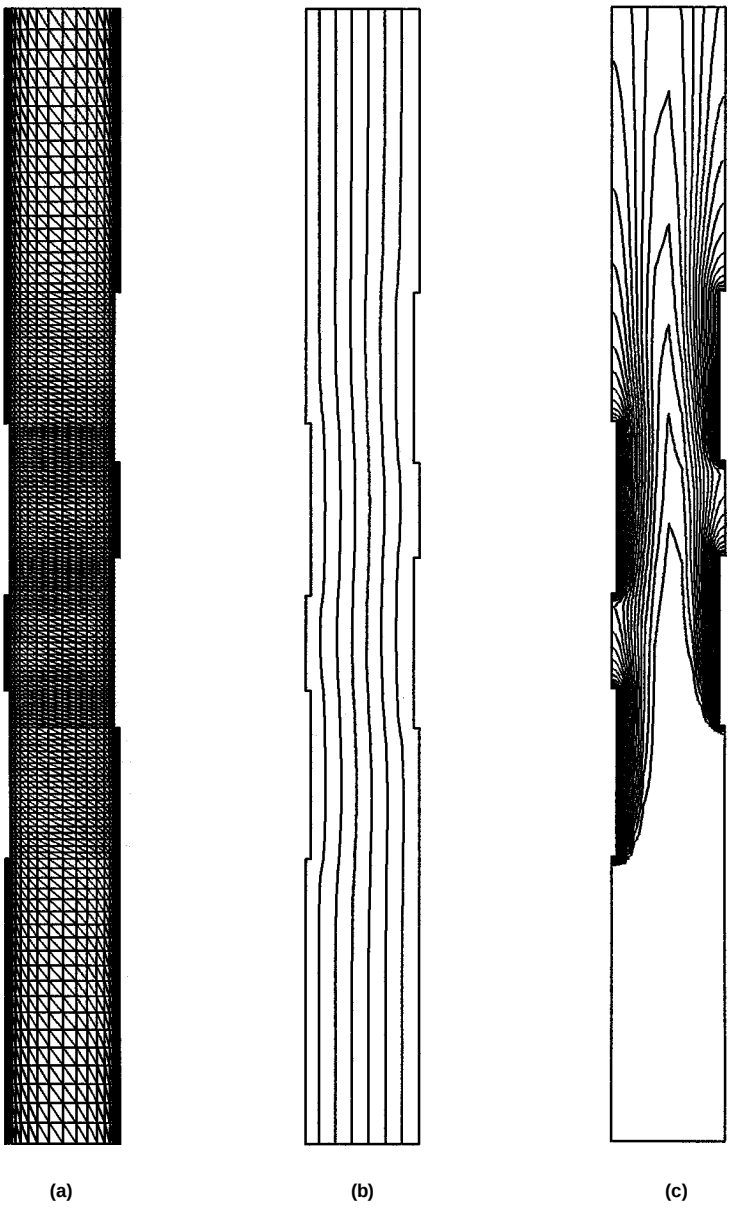

Figure 17.
Staggered plates, $W = 0.2$, $Ra = 5 \times 10^5$: (a) finite element mesh, no. nodes: 2,640; no. elements: 4,928; (b) stream lines; (c) isotherms

Natural convection from staggered vertical plates

This problem applies to the design of many devices used in energy conversion, and in electronic components. A typical geometry for such devices is shown in Figure 15, the domain of interest and the boundary conditions used are also presented in this figure. Characteristic dimension of the problem here is the

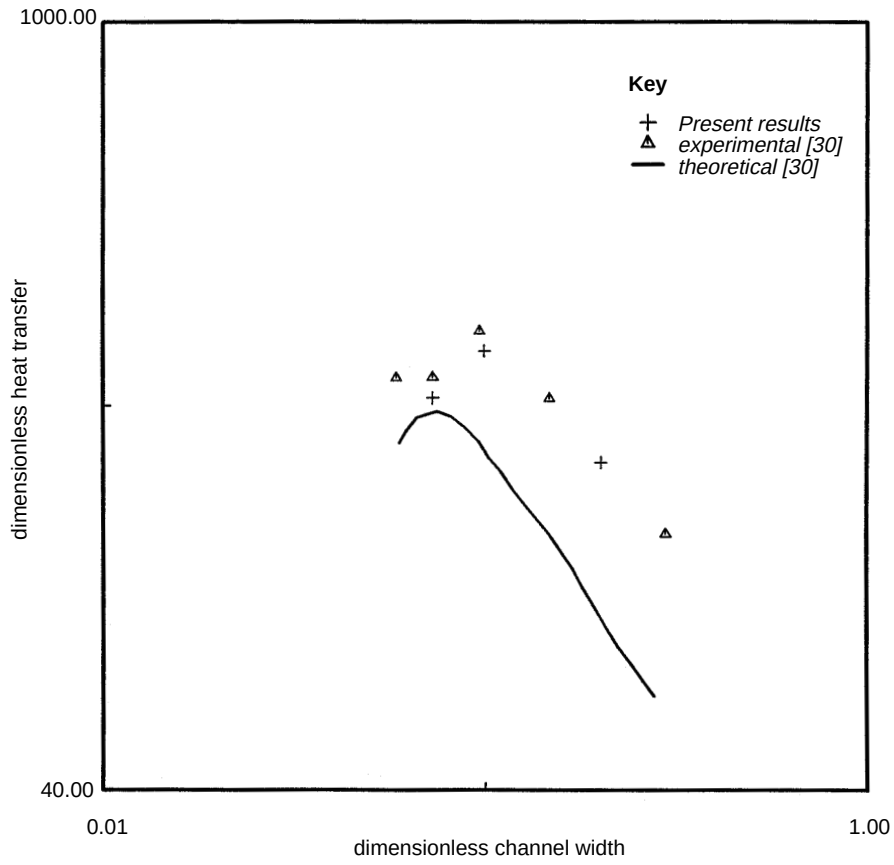

Figure 18.
Comparison of the dimensionless heat transfer with experimental and numerical data

Source: [30]

height of the channel L. The hot plates heat the surrounding fluid, which produces a variation in density and this induces flow in the channel due to buoyancy. In this study, calculations have been carried out for different Rayleigh numbers; for Ra = 5×10^5 and with of the channel W = 0.1 streamlines and isotherms are shown in Figure 16 together with the finite element mesh. Similar results, shown in Figure 17 correspond to W = 0.2. In fact it has already been pointed out by Ledezma and Bejan[30] that this dimension has an optimal value which maximise the heat transfer from the plates. The dimensionless parameter introduced to perform such optimization was:

$$\tilde{q} = \frac{q}{W(T_h - T_c)kB/L}$$

where q is the heat transfer rate for the channel, k the thermal conductivity of the fluid and B the length of the plates in the direction perpendicular to the x and y plane. The comparison between present and experimental results is

presented in Figure 18. The agreement is seen to be excellent and is much better than the results predicted by Ledezma and Bejan[30].

Conclusions

The Characteristic-Based-Split algorithm (CBS) has been applied to many thermal flow problems in its semi-implicit form. From a comparison of the results obtained with those available in literature (both experimental and theoretical) it is proved that the scheme performed excellently in solving these problems. In fact the agreement is excellent especially when the equations are coupled together via buoyancy term in the momentum equation. It is also proved that the present algorithm can be used to solve complicated heat transfer problems very accurately.

References

1. Zienkiewicz, O.C. and Codina, R., "A general algorithm for compressible and incompressible flow, Part I. The split characteristic based scheme", *Int. J. Num. Meth. Fluids*, Vol. 20, 1995, pp. 869-85.
2. Zienkiewicz, O.C., Satya Sai, B.V.K., Morgan, K., Codina, R. and Vázquez, M., "A general algorithm for compressible and incompressible flow – Part II. Tests on the explicit form", *Int. J. Num. Meth. Fluids*, Vol. 20, 1995, pp. 887-913.
3. Codina, R., Vázquez, M. and Zienkiewicz, O.C., "General algorithm for compressible and incompressible flows, Part III – A semi-implicit form", *Int. J. Num. Meth. Fluids*, Vol. 7, 1998, pp. 12-32.
4. Codina, R., Vázquez, M. and Zienkiewicz, O.C., An implicit fractional step finite element method for incompressible and compressible flows, *Proc. 10th Int. Conf. Finite Elements Fluids,* 5-8 January 1998, pp. 519-24.
5. Zienkiewicz, O.C. and Taylor, R.L., "The finite element method", Vol. 2, 4th ed., McGraw-Hill Book Company, New York, NY.
6. Oden, J.T. and Wellford, L.C., "Analysis of flow of viscous fluids by finite element method", *AIAA Journal,* Vol. 10, 1972, pp. 1590-9.
7. Taylor, C. and Hood, P., "A numerical solution of the Navier-Stokes equations using the finite element technique", *Comp. fluids,* Vol. 1, 1973, pp. 73-100.
8. Zienkiewicz, O.C., Gallagher, R.H. and Hood, P., "Newtonian and non-newtonian viscous incompressible flow temperature induced flows. Finite element solutions", in Whiteman, J. (Ed.), *Mathematics of Finite Elements and Application*, Vol. II, Academic Press, New York, NY, 1976, Ch. 20, pp. 235-67.
9. Christies, I., Griffiths, D.F., Mitchell, A.R. and Zienkiewicz, O.C., "Finite element methods for second order differential equations with significant first derivatives", *Int. J. Num. Meth. Engng.*, Vol. 10, 1976, pp. 1389-96.
10. Heinrich, J.C., Huyakorn, P.S., Mitchell, A.R. and Zienkiewicz, O.C., "An upwind finite element scheme for two-dimensional convective transport equation", *Int. J. Num. Meth. Engng.*, Vol. 11, 1977, pp. 131-44.
11. Courant, R., Isaacson, E. and Rees, M., "On the solution of non-linear hyperbolic differential equations by finite differences", *Comm. Pure Appl. Math.,* Vol. V, 1952, pp. 243-55.
12. Spalding, D.B., "A novel finite difference formulation for differential equations involving both first and second derivatives", *Int. J. Num. Meth. Engng.*, Vol. 4, 1972, pp. 551-9.
13. Hughes, T.J.R. and Brooks, A.N., "A multi-dimensional upwind scheme with no cross wind diffusion", in Hughes, T.J.R. (Ed.), *Finite Elements for Convection Dominated Flows,* AMD 34, ASME, 1979.

14. Kelly, D.W., Nakazawa, S. and Zienkiewicz, O.C., "A note on anisotropic balancing dissipation in the finite element approximation to convective diffusion problems", *Int. J. Num. Meth. Engng.,* Vol. 11, 1977, pp. 1831-44.
15. Donea, J.A., "Taylor-Galerkin method for convective transport problems", *Int. J. Num. Meth. Engng*, Vol. 20, 1984, pp. 101-19.
16. Lohner, R., Morgan K. and Zienkiewicz. O.C., "The solution of non-linear hyperbolic equation systems by the finite element method", *Int. J. Num. Meth. Fluids*, Vol. 4, 1984, pp. 1043-63.
17. Hughes, T.J.R., Franca, L.P. and Balastra, M., "A new finite element formulation for computational fluid dynamics: V. Circumventing the Babu check ska-Brezzi condition: a stable Petrov-Galerkin formulation of the Stokes problems accommodating equal-order interpolations", *Comp. Methods Appl. Mech. Eng.*, Vol. 59, 1986, pp. 85-99.
18. de Sampaio, P.A.B., "A Petrov-Galerkin formulation for the incompressible Navier-Stokes equations using equal order interpolation for velocity and pressure", *Int. J. Num. Meth. Engng.,* Vol. 31, 1991, pp. 1135-49.
19. Schneider, G.E., Raithby, G.D. and Yovanovich, M.M., "Finite element analysis of incompressible fluid flow incorporating equal order pressure and velocity interpolation", in Taylor, C., Morgan, K. and Brebbia, C.A. (Eds), *Numerical Methods in Laminar and Turbulent Flow*, Pentech, 1978.
20. Kawahara, M. and Ohmiya, K., "Finite element analysis of density flow using the velocity correction method", *Int. J. Num. Meth. Fluids*, Vol. 5, 1985, pp. 308-23.
21. Zienkiewicz, O.C. and Wu, J., "Incompressibility without tears – how to avoid the restrictions on mixed formulation", *Int. J. Num. Meth. Engng.,* Vol. 32, 1991, pp. 1189-203.
22. Chorin, A.J., "Numerical solution of the Navier-Stokes equations", *Math. Comput.,* Vol. 23, 1968, pp. 341-54.
23. Zienkiewicz, O.C. and Wu, J., "A general explicit of semi-explicit algorithm for compressible and incompressible flows", *Int. J. Num. Meth. Engng.*, Vol. 35, 1992, pp. 457-79.
24. Zienkiewicz, O.C., Satya Sai, B.V.K., Morgan, K. and Codina, R., "Split characteristic based semi-implicit algorithm for laminar/turbulent incompressible flows", *Int. J. Num. Meth. Fluids*, Vol. 23, 1996, pp. 787-809.
25. Codina, R., "Stability analysis of forward Euler scheme for the convection diffusion equation using the SUPG formulation in space", *Int. J. Num. Meth. Engng.*, Vol. 36, 1993, pp. 1445-64.
26. de Vahl Davis, D., "Natural convection of air in a square cavity: a bench mark numerical solution", *Int. J. Num. Meth. Fluids*, Vol. 3, 1983, pp. 249-64.
27. Le Quere, P. and De Roquefort, T.A., "Computation of natural convection in two dimensional cavity with Chebyshev polynomials", *J. Comp. Phys.*, Vol. 57, 1985, pp. 210-28.
28. Denham, M.K. and Patrick, M.A., "Laminar flow over a downstream facing step in a two dimensional channel", *Trans. Inst. Chem. Engrs.*, Vol. 52, 1974, pp. 361-7.
29. Kondon, T., Nagano, Y. and Tsuji, T., "Computational study of laminar heat transfer downstream a backward-facing step", *Int. J. Heat Mass Transfer,* Vol. 36, 1993, pp. 577-91.
30. Ledezma, G.A. and Bejan, A., "Optimal geometric arrangement of staggered vertical plates in natural convection", *ASME J. Heat Transfer*, Vol. 119, 1997, pp. 700-8.